Topological bimeronic beams

YIJIE SHEN

Optoelectronics Research Centre, University of Southampton, Southampton SO17 1BJ, United Kingdom

y.shen@soton.ac.uk

Compiled June 21, 2021

A family of structured light, namely bimeronic beams, was proposed to characterize the sophisticated topological structures of bimeron, the quasiparticle homeomorphic to skyrmion. The vector nature of bimeronic beams is not only reconfigurable by tuning topological numbers, unveiling a new mechanism to transform diverse topologies of light (akin to the topological transformations of skyrmion among Néel-, Bloch-, and anti-skyrmion types), but also more generalized to include skyrmionic transformations as simple cases.

http://dx.doi.org/10.1364/ao.XX.XXXXXX

Optical quasiparticles, using optical field to emulate salient quasiparticle properties from particle physics and condensed matter, are potential research directions attracting growing attentions as it enables new dimensions to control structured light and light–matter interactions [1–3]. Among them are optical skyrmions with sophisticated vectorial structures and topological protections, which was first generated in a structured electric field of evanescent wave [4], and subsequently constructed by the spin vectors of confined freespace waves [5, 6], Stokes vectors of paraxial vector beams [7, 8], and pseudospins in photonic crystals [9]. These optical skyrmions have promised advanced applications such as nanometer- and femtosecond-scale metrology [3], deep-subwavelength microscopy [5], ultrafast vector imaging [10], and topological Hall effects [9], broadening the frontier of modern fundamental and applied physics. While skyrmion is just a simple member in the great quasiparticle family [1], great endeavors are still pursuit to create more kinds of optical quasiparticles with generalized topological properties. For instances, skyrmioniums with multi-twist topologies were recently controlled on metasurface plasmons [11], some meron and second-order meron structures were reported in plasmonic field [3] and optical microcavities [12], respectively. Bimerons and bimeroniums are also very important quasiparticles emerged in recent years, that possess robust topological textures homeomorphic to skyrmions and offer promising features for advanced information processing, transport and storage [13–16]. However, the optical bimeron has never been reported yet.

In this Letter, a new quasiparticle state of light, optical bimeron(ium), is constructed by a family of structured vector beams. The bimeronic beams possess bimeron-like structures in their Stokes vector fields, which can be transformed to diverse generalized topological textures, including all the intermmediate skyrmionic states among Néel-, Bloch-, and anti-skyrmion types as simple members. Moreover, a graphical model is proposed to universally represent the complete topological evolution of tunable bimeronic beams onto a 3D Poincaré-like sphere. Finally, the propagation dynamics of bimeronic beams is also discussed.

Topological properties of a quasiparticle configuration can be characterized by the skyrmion number [1]:

$$s = \frac{1}{4\pi}\iint_{\sigma} \mathbf{n}\cdot\left(\frac{\partial \mathbf{n}}{\partial x}\times\frac{\partial \mathbf{n}}{\partial y}\right)\mathrm{d}x\mathrm{d}y \tag{1}$$

where $\mathbf{n}(x,y)$ represents the vector field to construct a quasiparticle and σ the region to confine it. The skyrmion number is usually treated as an integer that counts how many times the vector $\mathbf{n}(x,y) = \mathbf{n}(r\cos\phi, r\sin\phi)$ wraps around an unit sphere, with longitude and latitude angles noted as (α,β). For an example of a skyrmion of $s = 1$, the unit sphere mapping is shown as Fig. 1(a), where the sets of vectors from skyrmion center to boundary are mapped onto the spiny sphere from south pole to north pole, accordingly. Bimeron, a topological transition state of skyrmion, can also be described by the unit sphere mapping but changing wrapping style, as exemplified in Fig. 1(b) for the same spiny sphere and skyrmion number but the coordinates of longitude, latitude, and poles are switched. Based on the mapping, the quasiparticle vectors can be given by $\mathbf{n} = (\cos\alpha(\phi)\sin\beta(r), \sin\alpha(\phi)\sin\beta(r), \cos\beta(r))$, and the skyrmion number can be separated into additional topological numbers:

$$\begin{aligned} s =& \frac{1}{4\pi}\int_0^{r_\sigma}\mathrm{d}r\int_0^{2\pi}\mathrm{d}\phi\frac{\mathrm{d}\beta(r)}{\mathrm{d}r}\frac{\mathrm{d}\alpha(\phi)}{\mathrm{d}\phi}\sin\beta(r) \\ =& \frac{1}{4\pi}[\cos\beta(r)]_{r=0}^{r=r_\sigma}[\alpha(\phi)]_{\phi=0}^{\phi=2\pi} = p\cdot m \end{aligned} \tag{2}$$

the polarity, $p = \frac{1}{2}[\cos\beta(r)]_{r=0}^{r=r_\sigma}$, means that the vector direction is down (up) at center $r = 0$ and up (down) at boundary $r \to r_\sigma$ for $p = 1$ ($p = -1$), and the vorticity, $m = \frac{1}{2\pi}[\alpha(\phi)]_{\phi=0}^{\phi=2\pi}$, controls distribution of the transverse field components. For distinguishing diverse helical distributions, an initial phase γ should be added, $\alpha(\phi) = m\phi + \gamma$. These topological numbers provide a classic zoology of skyrmions. For the case of $m = 1$, the skyrmions of $\gamma = 0$ and $\gamma = \pi$ are classified as *Néel-type* that shows a hedgehog texture around the quasiparticle texture, and skyrmions of $\gamma = \pm\pi/2$ are *Bloch-type* with a vortex around the center, while the case of $m = -1$ is always defined as *anti-skyrmion* with a saddle texture, see first row of Fig. 1(c).

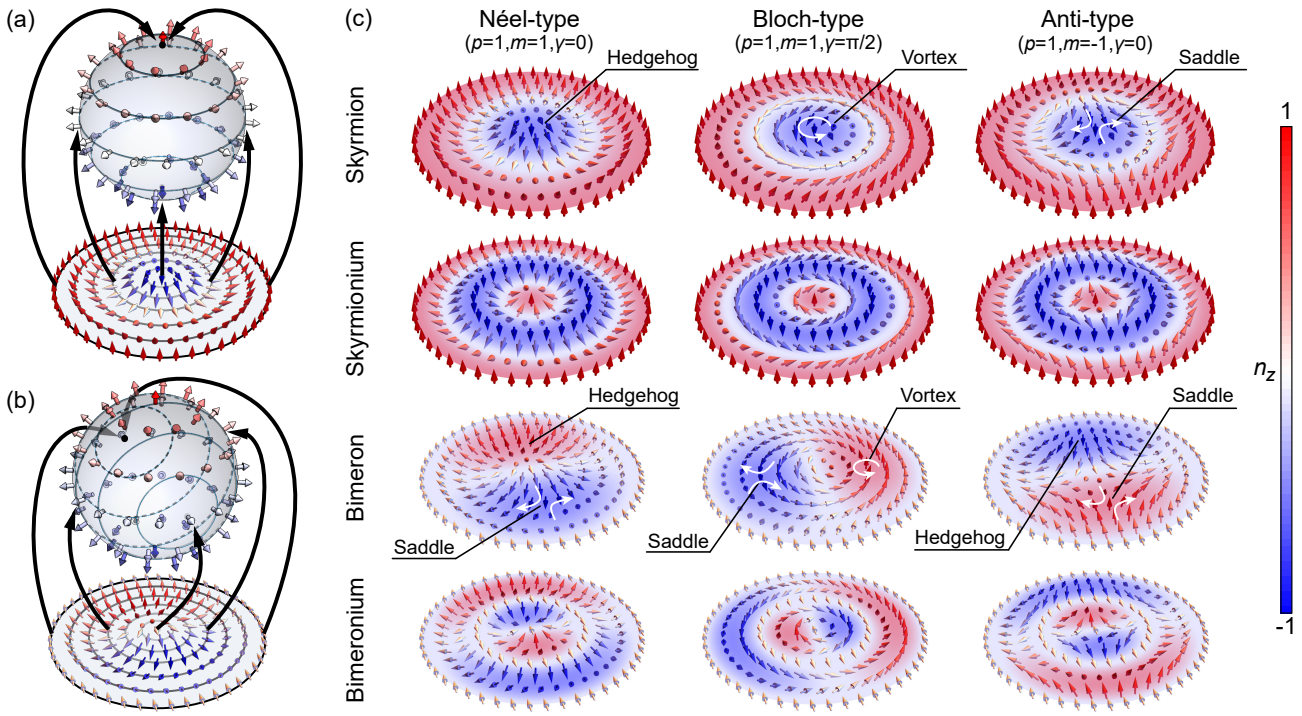

Fig. 1. (a-b) Representations of unit sphere mapping for skyrmion and bimeron, where the gray-gradient circles mark the latitude lines set on unit spheres and the sets of vectors of quasiparticle to map correspondingly. (c) Quasiparticle zoo accommodating skyrmions, skyrmioniums, bimerons, bimeroniums with their topological classifications of Néel-, Bloch-, and anti-types.

In addition to skyrmions, many new members were emerged in quasiparticle family with important roles in recent few years [1]. An immediate derivant of skyrmion is the skyrmionium, a coupled state of two decomposed skyrmions with opposite polarities, or more decomposed skyrmions showing radially multi-twist configuration (also named target skyrmion) [11], which can also be classified as Néel-, Bloch-, and anti-type topologies, just with higher-order radial structures, see second row of Fig. 1(c). The bimeron, as a generalized topologically transformed state of skyrmion, has the texture composed by two half-skyrmions (merons) with opposite polarities [15], where the prior topological zoology is also applicable. The third row of Fig. 1(c) show three topological bimerons, parallel to the three topological skyrmions, the Néel-type bimeron holds a hedgehog polarity-up meron and saddle polarity-down meron, the Bloch-bimeron an up-vortex and a down-saddle, and the anti-bimeron an up-saddle and a down-hedgehog. Very recently, a new concept of bimeronium was proposed as a derivant of bimeron [16], akin to the skyrmionium evolved from skyrmion. Similarly, a topological zoology of bimeronium is shown in fourth row of Fig. 1(c).

Optical skyrmions were recently constructed by the polarization Stokes vector fields of a set of customized vector beams, namely skyrmionic beams, which can be given by [7]:

$$|\Psi(\mathbf{r})\rangle = \mathrm{LG}_{0,0}(\mathbf{r})|R\rangle + e^{i\theta}\mathrm{LG}_{0,1}(\mathbf{r})|L\rangle \tag{3}$$

where $\mathbf{r} = (x, y, z)$, (x, y) represent transverse plane coordinates, and z is longitudinal coordinate, $\mathrm{LG}_{n,\ell}$ is the Laguerre-Gaussian mode with radial and azimuthal indices (n, ℓ), $|R\rangle$ and $|L\rangle$ are states of right- and left-handed circular polarizations, and the phase angle θ decides the topological texture of optical skyrmion. A skyrmionic beam possesses a spatial distribution of Stokes vectors $\mathbf{s} = (s_1, s_2, s_3)$ at focused plane ($z = 0$), which exactly has a skyrmionic texture controlled as Néel-type ($\theta = 0$ or π) and Bloch-type ($\theta = \pm\pi/2$), but excluding anti-skyrmion. Here a generalization is proposed to include anti-skyrmion as special case:

$$|\Psi(\mathbf{r})\rangle = \mathrm{LG}_{0,0}(\mathbf{r})|R\rangle + \mathrm{OAM}(\mathbf{r}|\theta, \varphi)|L\rangle \tag{4}$$

where the left-handed polarized component is replaced by the orbital angular momentum (OAM) Poincaré sphere beam, parameterized by longitude and latitude (θ, φ) of Poincaré sphere [17]:

$$\mathrm{OAM}(\mathbf{r}|\theta, \varphi) = \cos\varphi e^{i\theta}\mathrm{LG}_{0,1}(\mathbf{r}) + \sin\varphi \mathrm{LG}_{0,-1}(\mathbf{r}) \tag{5}$$

The prior skyrmionic beams, Eq. (3), is accommodated by Eq. (4) as special cases of $\varphi = 0$. The cases of $\varphi = \pm\pi/2$ are corresponding to anti-skyrmion, but this form still cannot represent bimeronic cases. I propose a further generalization to this end:

$$|\Psi(\mathbf{r})\rangle = \mathrm{LG}_{0,0}(\mathbf{r})|R\rangle + \mathrm{OAM}(\mathbf{r}|\theta, \varphi)|\psi\rangle \tag{6}$$

here, in contrast to Eq. (4), the left-handed polarization is replaced by arbitrary polarization:

$$|\psi\rangle = \cos\delta e^{i\epsilon}|R\rangle + \sin\delta|L\rangle \tag{7}$$

which, for instance of $\delta = \pi/4$ and $\epsilon = 0$, is reduced into horizontally polarization $|\psi\rangle = |H\rangle$. When $\delta = \pi/2$ and $\epsilon = 0$ ($|\psi\rangle = |L\rangle$), Eq. (6) is reduced into skyrmionic beam form of Eq. (4). When $\delta = \epsilon = 0$ ($|\psi\rangle = |R\rangle$), Eq. (6) is reduced into a scalar beam without quasiparticle texture. When δ is between 0 and $\pi/4$, Eq. (6) represents a general bimeronic beam. For other cases, Eq. (6) very generally represents topological bimeronic beams. The right-upper part of Fig. 2 shows the typical topological states of the bimeronic beams with the distributions of polarization and Stokes vector, respectively.

The model of bimeronic beams can easily be further generalized to include the cases of bimeronium and skyrmionium (or

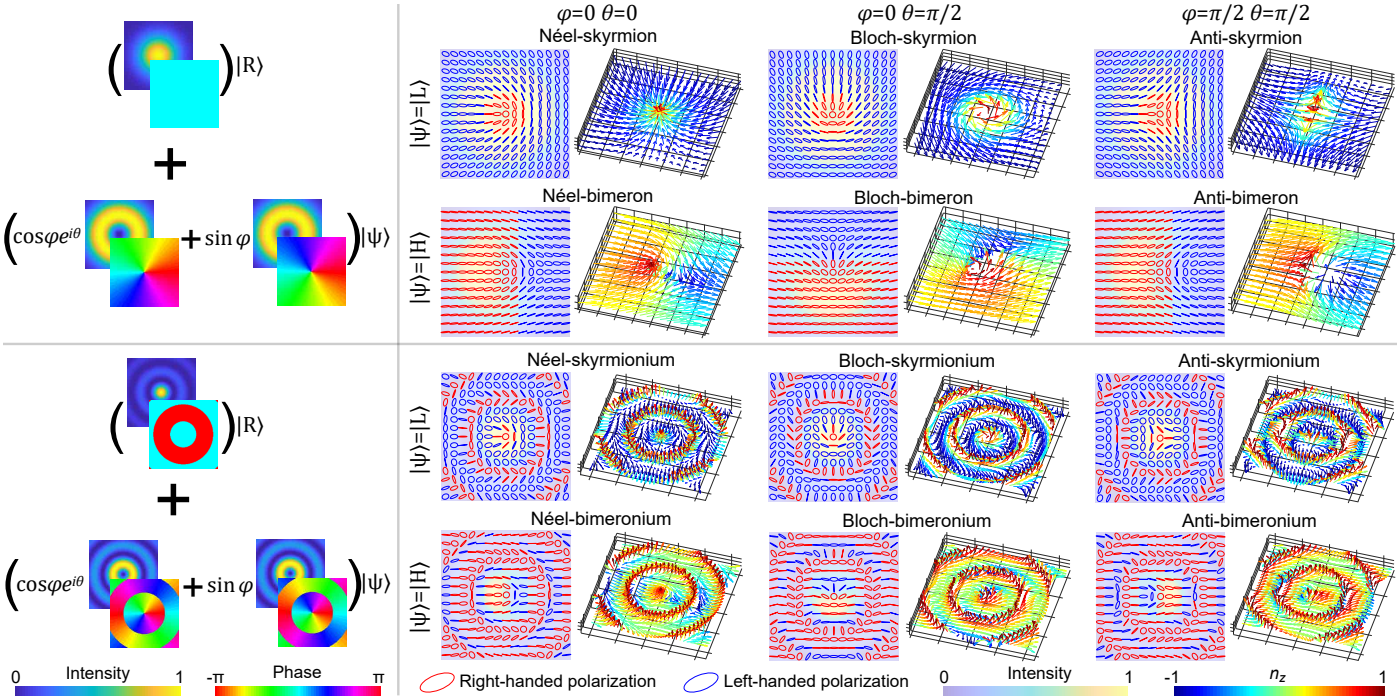

Fig. 2. Left: the conceptual structured light construction of bimerionic and bimerioniumic beams with decomposed LG and Bessel modes respectively; right: the distributions of intensity, polarization and Stokes vector at focus plane of bimerionic and bimerioniumic beams, classified by various topological states of Néel-, Bloch-, and anti-types, with parameters noted correspondingly.

target skyrmion). To this end, we can exploit the $\mathrm{LG}_{n,\pm1}$ modes with increasing radial index ($n \geq 1$) or Bessel beams [18], which have same OAM effects, also hold unique radially multi-π-step phase structure ($\mathrm{LG}_{n,\pm1}$ modes have n-times π-steps, Bessel mode theoretically infinite π-steps). The high-radial-index phase structure shows the evidence to be used to build the radially multi-π-twisted vector structure of bimeronium or skyrmionium. If we replace the $\mathrm{LG}_{0,\pm1}$ modes into high-radial-index OAM modes, the results will change into skyrmionium and bimeronium states, correspondingly, as the lower part of Fig. 2.

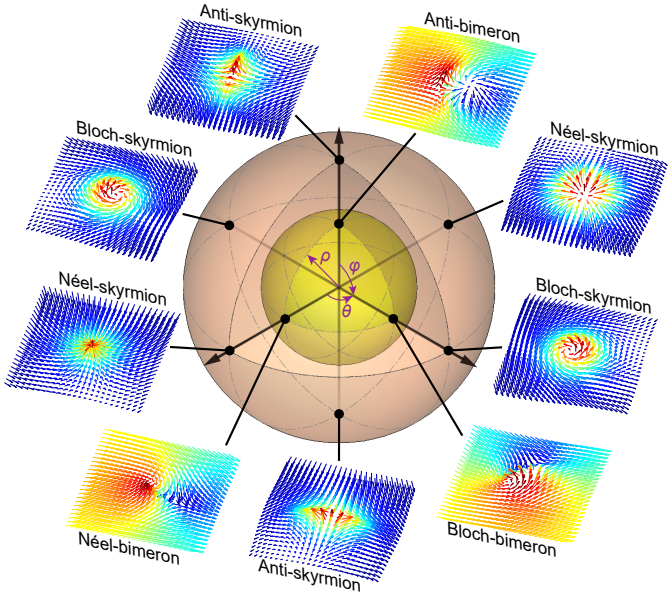

Fig. 3. Mapping of bimeronic beams onto a 3D Poincaré-like sphere, which shows complete transformations among bimerons with diverse topological textures: typical skyrmions and bimerons on selected points are shown.

Hereinafter, I present a graphical representation to characterize the complete topological transformation of the general bimerionic beams as Fig. 3. According to the mapping of OAM Poincaré sphere, $\mathrm{OAM}(\mathbf{r}|\theta,\varphi)$, that reveals modal evolution from non-OAM (at equator) to pure-OAM state (at two poles), we can map the general skyrmionic beams, Eq. (4), onto a Poincaré-like sphere with a unit radius $\rho = 1$. The equator represents Néel- and Bloch-type skyrmions and intermediate skyrmions between them with tuned helicity. The two poles stand for two anti-skyrmions with orthogonal orientations. Other region reveals the topological transition states with skyrmion number evolution (e.g., from $s = 1$ at equator to $s = -1$ at poles, the case in Fig. 3), akin to the OAM evolution. In addition, the general bimerionic beams, Eq. (6), for a given value of δ, are mapped on a inner sphere of radius $\rho = \tan(\delta/2)$ ($0 < \rho < 1$), again, the equator represents Néel- and Bloch-type and intermediate bimerons and the poles anti-bimerons. The center of sphere, $\rho = 0$, reveals the non-quasiparticle scalar field. Then all points in the solid sphere are mapped to bimeronic beams completely, an arbitrary route in the sphere reveals a topological transformation of the general bimeron. Such 3D Poincaré-like sphere for bimeronic beams provides not only a vivid understanding of its topology but also a potential toolkit to study deeper properties of geometric phase and spin-to-orbital conversion in the future.

In prior work, the propagation of a skyrmionic beam was studied, that shows a Bloch-type vector texture can evolve into Néel-type upon its propagation [7]. Here I show the bimeronic beams hold the similar topology-dependent propagation dy-

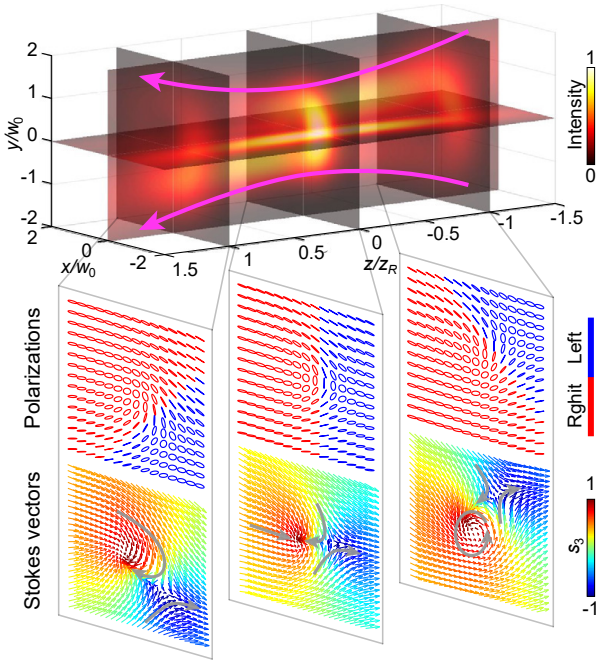

Fig. 4. Propagation dynamics of a bimerionic beam: the vector texture evolves from Bloch-type to Néel-type when the beam propagates through the Rayleigh range. The patterns of polarization and Stokes vector are plotted at the three propagation distances, $z = 0$ and $z = z_R$, of the beam, respectively.

namics. The result of a bimeronic beam ($\varphi = 0, \theta = 0, \delta = \pi/4$) is shown in Fig. 4, with spatial intensity pattern and distributions of polarization and Stokes vector at different propagation distances, $z = 0$ (at focus) and $z = \pm z_R$ (z_R is Rayleigh length). The bimeronic texture evolves from a Bloch-type ($z = -z_R$), into Néel-type at focus, then gradually into a intermediate state ($z = -z_R$). Therefore, in contrast to conventional vector beams, bimeronic beams have salient longitudinal-variant vector patterns with elegant topological characterization, which meets what urgently demanded in higher-dimensional structured light control for breaking current technical limits [19, 20].

Besides the above results of topological bimerons under only unit vorticity ($m = \pm 1$), there are still a large group of topological quasiparticles to be explored with wide prospect to extend. For instance, we can further exploit OAM modes with larger topological charge (value of $|\ell|$) to explore higher-order skyrmionic or bimeronic structures. Also, recent advance of structured light has promised many novel kinds of multi-singularity OAM modes [21], being as resource to be used for creating optical quasiparticles. On the other hand, new quasiparticles in condensed or magnetic matter were continually proposed and observed with increasingly complex topology, such as skyrmion bag [22], meron lattices [23], polar meron [24], and Hopfions [25], which provide open challenges to create and control corresponding optical quasiparticles towards general topological tunability of light.

In conclusion, the first optical analog of bimeron, i.e. bimeronic beams, is presented by a family of customized vector beams. The topological textures of bimeronic beams can be tunable and transformed into diverse Néel-, Bloch-, and anti-types, accommodating prior skyrmionic topologies as simple members. The complete topological transformation can be represented by an elegant 3D Poincaré-like sphere. The new topological state of light introduces more generalized quasiparticle methodologies into structured light control with more degrees of freedom, opening new dimensions for information processing and light-matter interaction.

Acknowledgement. The author thinks Xichao Zhang and Ziyu Zhan for useful discussions.

Disclosures. The author declares no conflicts of interest.

REFERENCES

1. B. Göbel, I. Mertig, and O. A. Tretiakov, Phys. Reports **895**, 1 (2021).
2. N. Rivera and I. Kaminer, Nat. Rev. Phys. **2**, 538 (2020).
3. Y. Dai, Z. Zhou, A. Ghosh, R. S. Mong, A. Kubo, C.-B. Huang, and H. Petek, Nature **588**, 616 (2020).
4. S. Tsesses, E. Ostrovsky, K. Cohen, B. Gjonaj, N. Lindner, and G. Bartal, Science **361**, 993 (2018).
5. L. Du, A. Yang, A. V. Zayats, and X. Yuan, Nat. Phys. **15**, 650 (2019).
6. R. Gutiérrez-Cuevas and E. Pisanty, J. Opt. **23**, 024004 (2021).
7. S. Gao, F. C. Speirits, F. Castellucci, S. Franke-Arnold, S. M. Barnett, and J. B. Götte, Phys. Rev. A **102**, 053513 (2020).
8. H. Kuratsuji and S. Tsuchida, Phys. Rev. A **103**, 023514 (2021).
9. A. Karnieli, S. Tsesses, G. Bartal, and A. Arie, Nat. Commun. **12**, 1 (2021).
10. T. J. Davis, D. Janoschka, P. Dreher, B. Frank, F.-J. M. zu Heringdorf, and H. Giessen, Science **368** (2020).
11. Z.-L. Deng, T. Shi, A. Krasnok, X. Li, and A. Alù, arXiv preprint arXiv:2104.02908 (2021).
12. M. Król, H. Sigurdsson, K. Rechcińska, P. Oliwa, K. Tyszka, W. Bardyszewski, A. Opala, M. Matuszewski, P. Morawiak, R. Mazur, W. Piecek, P. Kula, P. Lagoudakis, B. Pietka, and J. Szczytko, Optica **8**, 255 (2021).
13. B. Göbel, A. Mook, J. Henk, I. Mertig, and O. A. Tretiakov, Phys. Rev. B **99**, 060407 (2019).
14. L. Shen, J. Xia, X. Zhang, M. Ezawa, O. A. Tretiakov, X. Liu, G. Zhao, and Y. Zhou, Phys. Rev. Lett. **124**, 037202 (2020).
15. H. Jani, J.-C. Lin, J. Chen, J. Harrison, F. Maccherozzi, J. Schad, S. Prakash, C.-B. Eom, A. Ariando, T. Venkatesan, and P. Radaelli, Nature **590**, 74 (2021).
16. X. Zhang, J. Xia, M. Ezawa, O. A. Tretiakov, H. T. Diep, G. Zhao, X. Liu, and Y. Zhou, Appl. Phys. Lett. **118**, 052411 (2021).
17. Y. Shen, Z. Wang, X. Fu, D. Naidoo, and A. Forbes, Phys. Rev. A **102**, 031501 (2020).
18. O. C. Vicente and C. Caloz, Optica **8**, 451 (2021).
19. A. Forbes, M. de Oliveira, and M. R. Dennis, Nat. Photonics **15**, 253 (2021).
20. Y. Shen, I. Nape, X. Yang, X. Fu, M. Gong, D. Naidoo, and A. Forbes, Light. Sci. & Appl. **10**, 50 (2021).
21. Y. Shen, X. Wang, Z. Xie, C. Min, X. Fu, Q. Liu, M. Gong, and X. Yuan, Light. Sci. & Appl. **8**, 1 (2019).
22. D. Foster, C. Kind, P. J. Ackerman, J.-S. B. Tai, M. R. Dennis, and I. I. Smalyukh, Nat. Phys. **15**, 655 (2019).
23. X. Yu, W. Koshibae, Y. Tokunaga, K. Shibata, Y. Taguchi, N. Nagaosa, and Y. Tokura, Nature **564**, 95 (2018).
24. Y. Wang, Y. Feng, Y. Zhu, Y. Tang, L. Yang, M. Zou, W. Geng, M. Han, X. Guo, B. Wu, and X. Ma, Nat. Mater. **19**, 881 (2020).
25. I. Luk'Yanchuk, Y. Tikhonov, A. Razumnaya, and V. Vinokur, Nat. Commun. **11**, 1 (2020).